Moretti et al.

Supplementary Material

Supplementary Figure 1. SLY ChIP-Seq extended panel.

(A) Graphic representation of the percentage of SLY-enriched genomic regions (pink) and of the genome (blue) which are promoters (i.e. 1kb region upstream of TSS) calculated by Cis-regulatory Element Annotation System (CEAS). P-value for the significance of the relative enrichment with respect to the background was calculated using one-sided binomial test. (B) Graphic representation of the percentage of each chromosome found occupied by SLY protein by ChIP-Seq. (C) Results from ontology analyses of SLY ChIP-Seq genes using Genomatix.

Supplementary Figure 2. SLY co-localizes with active epigenetic marks.

(A) Graphic representation of ChIP-Seq profile showing the average enrichment of SLY, H3K4me3, Kcr, H3K27me3 and H3K9me3 around the TSS of genes expressed (in red) and not expressed (in black) in round spermatids. (B) Percentage of genes with SLY present at their TSS (TSS +/- 500bp) among all mouse genes (mm10 version, in black) or among different categories of genes which are deregulated in Sly-KD spermatids (green or red). For genes significantly deregulated more than 1.5 fold, a higher proportion of upregulated genes (most of them XY-encoded genes) *versus* downregulated genes was found (χ^2, p=0.005). When including all 1,171 significantly deregulated genes (no threshold, p<0.05), there were more downregulated than upregulated genes (χ^2, p=0.012). All downregulated genes are autosomal genes. See also Table 2.

Supplementary Figure 3. List of the genes with highest SLY peaks (Top 10%).

Supplementary Figure 4. DOT1L protein pattern of expression in WT and Sly-KD testicular sections.

Representative immunodetection images obtained using antibody against DOT1L protein on testicular sections from wild-type (WT) and Sly-knockdown (Sly-KD) mice, at stage XII (stage where DOT1L co-localizes with the sex body in spermatocytes), stage IV (where DOT1L is detected in round spermatids) and stage X (where DOT1L is detected in elongating spermatids). The black and white images represent DAPI staining of the nuclei. DOT1L was detected in green. Lectin (red) was used to stain acrosomes in order to determine tubule stage. No detectable changes in pattern of expression was observed in Sly-KD versus WT spermatids, but the intensity of DOT1L signal over background in elongating spermatids is lower in Sly-KD compared to WT sections (see also Supplementary Figure 5). The inset in the upper-right corner represents a 2-fold magnification of the region in the white square. 'CS' stands for condensing spermatids, 'SC' for spermatocytes, 'RS' for round spermatids and 'ES' for elongating spermatids. Scale bar indicates 20µm.

Supplementary Figure 5. DOT1L quantification by immunofluorescence.

Schematics showing immunofluorescence quantification of DOT1L signal in Sly-KD and WT elongating spermatids (A) and in Sly-KD and WT spermatocytes at stage XII (B). The graphs represent the mean level +/- standard error of means. The star indicates significant different between the two genotypes by t-test ($p<0.01$).

Supplementary Figure 6. H3K79me2 pattern of expression in WT and Sly-KD testicular sections.

Representative immunodetection images obtained using antibody against H3K79me2 on testicular sections from wild-type (WT) and Sly-knockdown (Sly-KD) mice, at stage XI and XII (where H3K79me2 is detected in elongating spermatids) and at stage IV (where H3K79me2 signal is detected in round spermatids). The black and white images represent DAPI staining of the nuclei. H3K79me2 was detected in green. Lectin (red) was used to stain acrosomes in order to determine tubule stage. Pictures were taken using the same image capture parameters. No detectable changes in term of timing of expression was observed in Sly-KD versus WT spermatids, however the intensity of H3K79me2 signal over background in elongating spermatids (stage XII and stage XI pictures) is markedly reduced in Sly-KD versus WT sections, as measured in Figure 4. Scale bar indicates 20μm.

Supplementary Figure 7. H3K79me2 quantification by western blot.

(A) Western blot detection of H3K79me2 in protein extracts from WT and Sly-KD (KD) elongating/condensing (ES/CS) spermatids. Antibody against TUBULIN was used to normalize the signal. Since the variability among samples from the same genotype was elevated we show here all the results we obtained in 3 independent experiments. (B) Western blot detection of H3K79me2 in protein extracts from WT and Sly-KD spermatozoa. A higher proportion of histones (notably of histone H3) is retained in Sly-KD spermatozoa compared to WT spermatozoa (see Figure 6), therefore, we also detected the same protein extracts with anti-Pan-H3 antibody. For both detection (H3K79me2 and Pan-H3), antibody against TUBULIN was used to normalize the signal. (C and D) Schematics showing western blot quantification of H3K79me2 (normalized to TUBULIN level) in Sly-KD and WT elongating/condensing spermatids (C) and in Sly-KD and WT spermatozoa (D). For spermatozoa, normalized H3K79me2 level was reported to that of normalized histone H3 level (detected with Pan-H3 antibody). On the scatter plots is represented the mean level +/- standard error of means. The star indicates significant different between the two genotypes by t-test [n = 7-8 samples per genotype, p=0.01 for (C); n= 4-5 samples per genotype, p=0.03 for (D)].

Supplementary Figure 8. H3K79me2 detection in spermatozoa.

Immunofluorescence detection of H3K79me2 (red) in WT epididymal spermatozoa. Hoechst (blue) was used to stain nuclei.

Supplementary Figure 9. AcH4 pattern of expression in WT and Sly-KD testicular sections.

Representative immunodetection images obtained using antibody against AcH4 on testicular sections from wild-type (WT) and Sly-knockdown (Sly-KD) mice, from stage X to XII. The black and white images represent DAPI staining of the nuclei. AcH4 was detected in green. Lectin (red) was used to stain acrosomes in order to determine tubule stage. Pictures were taken using the same image capture parameters. No detectable changes in pattern of expression was observed in Sly-KD versus WT spermatids, however the intensity of AcH4 signal over background in elongating spermatids (stage X to stage XII) is markedly reduced in Sly-KD versus WT sections, as measured in Figure 5. Scale bar indicates 20µm.

Supplementary Figure 10. Characterization of FLAG-SLY transgenic mice.

(A) Transcript level of *Sly1* isoform and of *Sly* all isoforms (Sly global) measured by RT-qPCR in wild-type (WT) and FLAG-SLY transgenic whole testes. The graph represents the mean +/- standard error of means (after normalization with *Acrv1*, n=4 samples per genotype). A significant difference between FLAG-SLY and WT samples was found by t-tests with both types of primers (p-value<0.0005). (B) Western blot detection of SLY protein in cytosolic and nuclear fractions of adult FLAG-SLY and WT testes, using anti-FLAG, anti-SLY and anti-SLX/SLXL1 antibodies. Anti-FLAG only detects FLAG-SLY recombinant protein. Anti-SLY detects endogenous SLY and FLAG-SLY recombinant protein. Anti-SLX/SLXL1 was used to control the purity of the nuclear fraction. Arrows indicate the specific band (at expected sizes of ~38kDa for SLY/FLAG-SLY, and ~34KDa for SLX/SLXL1) and stars, non-specific bands. Ponceau staining was used to control the quantity of protein loaded in each lane. (C) Immunodetection using antibody against FLAG on stage VII testicular sections from FLAG-SLY and WT mice. FLAG was detected in green. DAPI (in blue) was used to stain the nuclei. Lectin (red) was used to stain acrosomes in order to determine tubule stage. RS indicates 'round spermatids', SC indicates 'spermatocytes'. In the upper panel, the scale bar indicates 20µm. The bottom panel represents a 2x magnification of the insets. Pictures were taken using the same image capture parameters. The recombinant FLAG-SLY protein is only detected in FLAG-SLY transgenic round spermatids.

Supplementary Figure 11. List of the primers designed for the present study.

A

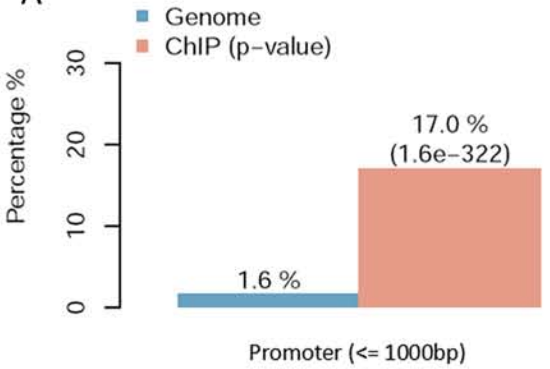

B

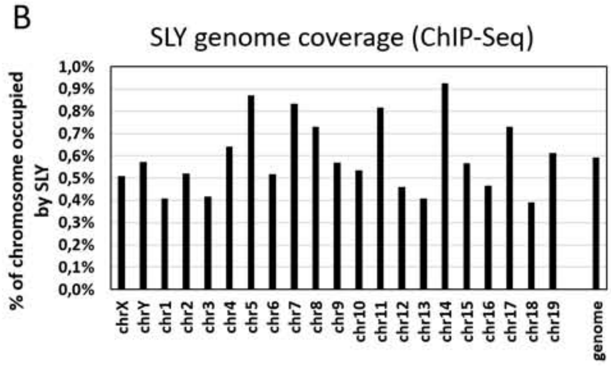

C

Genomatix ontology analysis of SLY ChIP-Seq genes

A

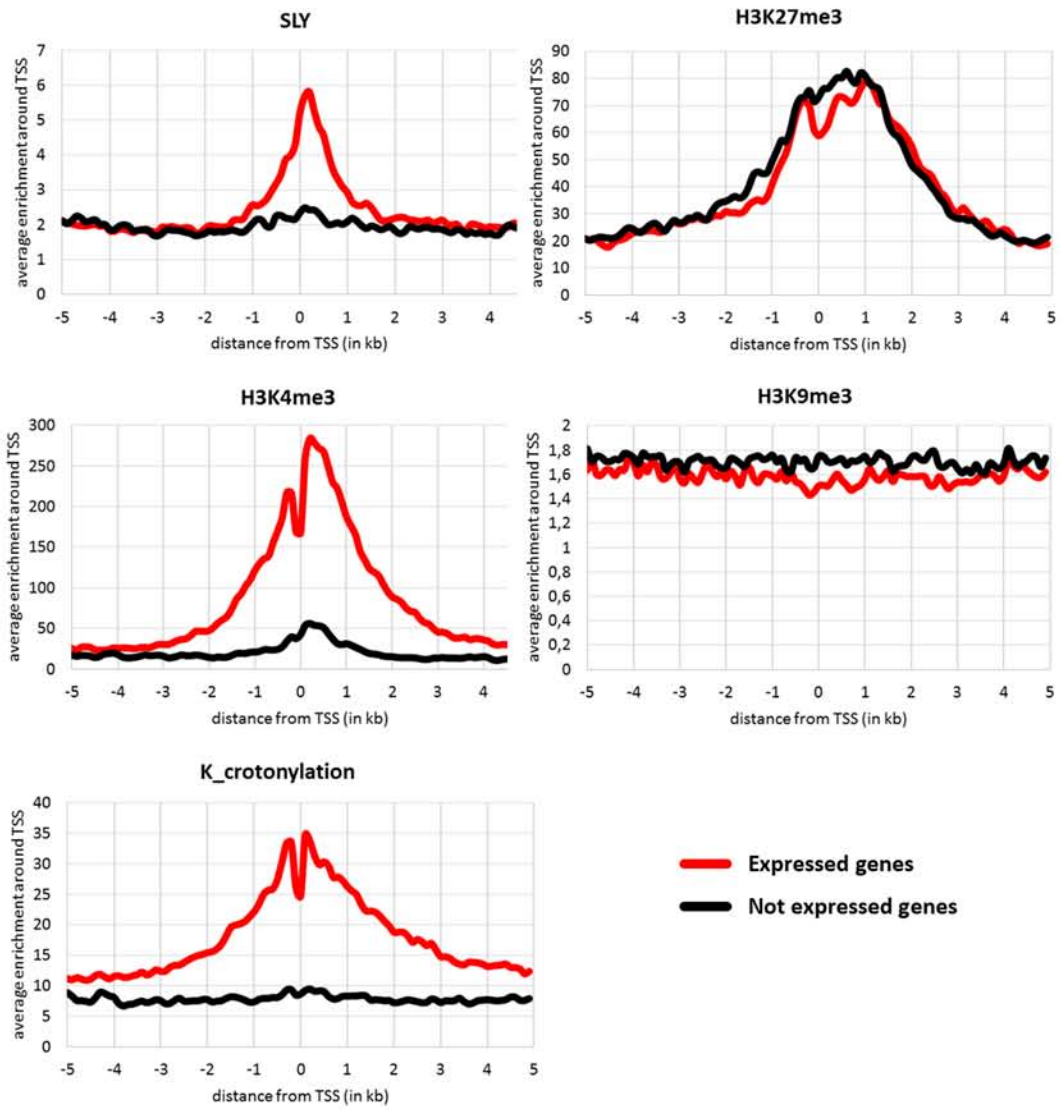
SLY
H3K27me3
H3K4me3
H3K9me3
K_crotonylation
average enrichment around TSS
distance from TSS (in kb)
Expressed genes
Not expressed genes

B

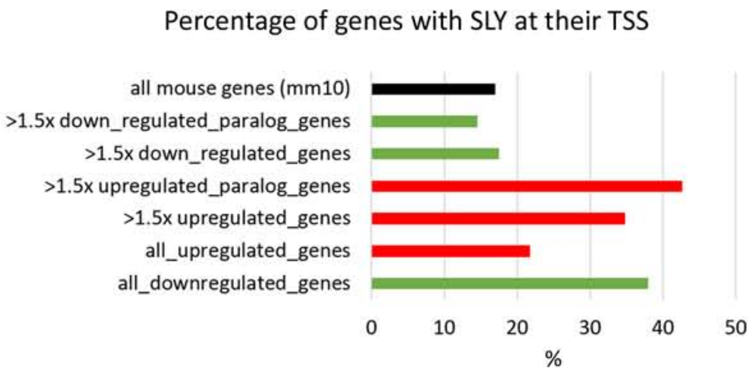
Percentage of genes with SLY at their TSS
all mouse genes (mm10)
>1.5x down_regulated_paralog_genes
>1.5x down_regulated_genes
>1.5x upregulated_paralog_genes
>1.5x upregulated_genes
all_upregulated_genes
all_downregulated_genes
0
10
20
30
40
50
%

Fig S3. Moretti et al.

chromosome location	gene name
chr1	4930594C11Rik
chr1	Abl2
chr1	Actr3
chr1	Boll
chr1	Desi2
chr1	Dis3l2
chr1	Dnah14
chr1	Efcab2
chr1	Fbxo28
chr1	Fbxo36
chr1	Fcgr3
chr1	Gm16067
chr1	Gm16094
chr1	Gm25911
chr1	Gpatch2
chr1	H3f3a
chr1	Hjurp
chr1	Inpp4a
chr1	Kdm5b
chr1	Lmbrd1
chr1	mmu-mir-6546
chr1	Pask
chr1	Ppp1r7
chr1	Prrc2c
chr1	Rc3h1
chr1	Sp110
chr1	Sp140
chr1	Spata17
chr1	Stk17b
chr1	Suco
chr1	Tor1aip1
chr1	Tor1aip2
chr1	Trip12
chr1	Trpm8
chr1	Zfp451
chr2	1700003F12Rik
chr2	2900097C17Rik
chr2	Adnp
chr2	Cse1l
chr2	Ddx31
chr2	Gabpb1
chr2	Gm10800
chr2	Gm10801
chr2	Gm11458
chr2	Gm13345
chr2	Gm13483
chr2	Gm13532
chr2	Gm23969

chromosome location	gene name
chr10	Ctdsp2
chr10	Ddx50
chr10	Dot1l
chr10	Dtx3
chr10	Eef2
chr10	F420014N23Rik
chr10	Fzr1
chr10	Gm8540
chr10	Gucd1
chr10	Jmjd1c
chr10	Lats1
chr10	Mex3d
chr10	Pcmt1
chr10	Pcnt
chr10	Pttg1ip
chr10	Rrp1
chr10	Snord37
chr10	Snrpd3
chr10	Snrpf
chr10	Speer5-ps1
chr10	Stk11
chr10	Uhrf1bp1l
chr11	1700016P03Rik
chr11	1700024J04Rik
chr11	1700064E03Rik
chr11	1700106J16Rik
chr11	Arhgap23
chr11	Cdk12
chr11	Cep95
chr11	Cltc
chr11	Csnk1d
chr11	Cyb5d1
chr11	Ddx5
chr11	Efcab5
chr11	Eif4a1
chr11	Epn2
chr11	Gas2l1
chr11	Gga3
chr11	Ggnbp2
chr11	Gm11423
chr11	Gm12061
chr11	Gm12204
chr11	Gm12206
chr11	Gm12209
chr11	Gm12279
chr11	Gsg2
chr11	Hexim2
chr11	Jmjd6

chr2	Gm27003	chr11	Kansl1
chr2	GNAS-AS1_4	chr11	Kpna2
chr2	GNAS-AS1_5	chr11	Lig3
chr2	Gtf3c4	chr11	Lsmd1
chr2	Med22	chr11	Med13
chr2	Mllt10	chr11	Mettl23
chr2	Mmadhc	chr11	Mir132
chr2	Naif1	chr11	Mir212
chr2	Nespos	chr11	Mnt
chr2	Ntmt1	chr11	Morc2a
chr2	Odf2	chr11	Mrps7
chr2	Ppp4r1l-ps	chr11	Msl1
chr2	Qsox2	chr11	Nploc4
chr2	Rab22a	chr11	Papolg
chr2	Rpl7a	chr11	Phf23
chr2	Slc25a25	chr11	Poldip2
chr2	Spo11	chr11	Ppp1r9b
chr2	Ttc30a1	chr11	Rptor
chr2	Ttc30b	chr11	Slc43a2
chr2	Zbtb34	chr11	Tekt3
chr2	Zfp335	chr11	Tlk2
chr3	1700125G22Rik	chr11	Tmem199
chr3	4930539J05Rik	chr11	Tmem88
chr3	4930577N17Rik	chr11	Tug1
chr3	4933429H19Rik	chr11	TUG1_1
chr3	Adad1	chr11	Ubb
chr3	Arnt	chr11	Ube2b
chr3	Atxn7l2	chr11	Ubtd2
chr3	Chtop	chr11	Ulk2
chr3	Ect2	chr11	Usp34
chr3	Elf2	chr11	Ybx2
chr3	Gar1	chr12	4930555J06Rik
chr3	Gm17402	chr12	Angel1
chr3	Gm20632	chr12	Arl4a
chr3	Hist2h2aa2	chr12	Cpsf2
chr3	Hist2h3c2	chr12	Crip2
chr3	Hspa4l	chr12	D130020L05Rik
chr3	Mfn1	chr12	Dcaf5
chr3	Mlf1	chr12	Eif5
chr3	Mtx1	chr12	Hsp90aa1
chr3	Naa15	chr12	Otub2
chr3	Pgrmc2	chr12	Pnpla8
chr3	Polr3c	chr12	Rab10
chr3	Pygo2	chr12	Rtn1
chr3	Rnf115	chr12	Smek1
chr3	Rsbn1	chr12	Tmed10
chr3	Sec62	chr12	Wdr20a
chr3	Thbs3	chr12	Yy1
chr3	Ube2d3	chr12	Zc3h14
chr4	1700095A21Rik	chr13	Arid4b

chr4	2610301B20Rik	chr13	BC005537
chr4	4933438K21Rik	chr13	Btf3
chr4	Akirin2	chr13	Fars2
chr4	D4Wsu53e	chr13	Ggps1
chr4	Fam229a	chr13	Gm24187
chr4	Fam76a	chr13	Gm9828
chr4	Gm10580	chr13	Hnrnpk
chr4	Gm12905	chr13	Lyrm4
chr4	Gm13034	chr13	Nup153
chr4	Gm13135	chr13	Rmi1
chr4	Gm13136	chr13	Rnf44
chr4	Gm13140	chr13	Ssr1
chr4	Gm13165	chr14	1700001F09Rik
chr4	Gm13169	chr14	1700049E17Rik1
chr4	Gm13231	chr14	1700049E17Rik2
chr4	Gm13236	chr14	1700091H14Rik
chr4	Gm13238	chr14	3110083C13Rik
chr4	Gm13241	chr14	4930444M15Rik
chr4	Gm13275	chr14	4931440J10Rik
chr4	Gm13278	chr14	BC061237
chr4	Gm13285	chr14	D14Abb1e
chr4	Gm13287	chr14	Ddhd1
chr4	Gm13288	chr14	Fgf9
chr4	Gm13289	chr14	Gm10128
chr4	Gm13290	chr14	Gm10340
chr4	Gm21953	chr14	Gm10375
chr4	Gm21980	chr14	Gm10376
chr4	Gm26525	chr14	Gm10377
chr4	Gm26606	chr14	Gm15918
chr4	Gm26763	chr14	Gm16241
chr4	Gm26867	chr14	Gm16506
chr4	Lrrc41	chr14	Gm17026
chr4	Mycbp	chr14	Gm17027
chr4	Pigv	chr14	Gm17078
chr4	Rbm12b1	chr14	Gm17079
chr4	Rbm12b2	chr14	Gm17093
chr4	Sfpq	chr14	Gm17124
chr4	Smarca5-ps	chr14	Gm17174
chr4	Spata6	chr14	Gm17175
chr4	Tmem222	chr14	Gm17654
chr4	Tmem67	chr14	Gm21560
chr4	Tssk3	chr14	Gm21738
chr4	Ube2j2	chr14	Gm21754
chr4	Uqcrh	chr14	Gm21977
chr4	Vcp	chr14	Gm2237
chr4	Zcchc11	chr14	Gm2832
chr4	Zfp37	chr14	Gm2930
chr5	4930449I24Rik	chr14	Gm2951
chr5	4930572O03Rik	chr14	Gm2974
chr5	5031410I06Rik	chr14	Gm3002

chr5	Abcf2
chr5	Adap1
chr5	Atxn2
chr5	D5Ertd579e
chr5	Dynll1
chr5	Erp29
chr5	Gm10220
chr5	Gm10354
chr5	Gm10382
chr5	Gm10471
chr5	Gm13830
chr5	Gm17019
chr5	Gm1979
chr5	Gm21655
chr5	Gm21671
chr5	Gm21698
chr5	Gm23866
chr5	Gm3402
chr5	Gm3409
chr5	Gm3415
chr5	Gm3495
chr5	Gm5862
chr5	Gm6272
chr5	Gm6370
chr5	Gm7347
chr5	Gm7361
chr5	Gm9758
chr5	Gtf2ird2
chr5	Iscu
chr5	Kctd10
chr5	Mlec
chr5	Nudt9
chr5	Nupr1l
chr5	Rab28
chr5	Radil
chr5	Sart3
chr5	Sfswap
chr5	Sgcb
chr5	Smim14
chr5	Spata18
chr5	Speer4a
chr5	Speer4b
chr5	Speer4c
chr5	Speer4d
chr5	Speer4e
chr5	Speer4f
chr5	Tmem116
chr5	Ubc
chr5	Ube2k
chr5	Ube3b

chr14	Gm3012
chr14	Gm3015
chr14	Gm3072
chr14	Gm3095
chr14	Gm3115
chr14	Gm3141
chr14	Gm3173
chr14	Gm3239
chr14	Gm3264
chr14	Gm3298
chr14	Gm3317
chr14	Gm3327
chr14	Gm3373
chr14	Gm3411
chr14	Gm3453
chr14	Gm3468
chr14	Gm3486
chr14	Gm3500
chr14	Gm3543
chr14	Gm3573
chr14	Gm3591
chr14	Gm3629
chr14	Gm3633
chr14	Gm3636
chr14	Gm3676
chr14	Gm3696
chr14	Gm4181
chr14	Gm5798
chr14	Gm5799
chr14	Gm5929
chr14	Gm6337
chr14	Gm6356
chr14	Gm6401
chr14	Gm6482
chr14	Gm7233
chr14	Gm7929
chr14	Gm7945
chr14	Gm7951
chr14	Gm7954
chr14	Gm7970
chr14	Gm7980
chr14	Gm8005
chr14	Gm8011
chr14	Gm8020
chr14	Gm8024
chr14	Gm8032
chr14	Gm8068
chr14	Gm8082
chr14	Gm8094
chr14	Gm8104

chr5	Wbscr27	chr14	Gm8108
chr5	Ythdc1	chr14	Gm8122
chr5	Zcchc8	chr14	Gm8126
chr6	1600020E01Rik	chr14	Gm8127
chr6	1700095J07Rik	chr14	Gm8138
chr6	4933440N22Rik	chr14	Gm8165
chr6	BC049715	chr14	Gm8180
chr6	Ccdc91	chr14	Gm8212
chr6	Chd4	chr14	Gm8220
chr6	Cntnap2	chr14	Gm8229
chr6	Gm24975	chr14	Gm8232
chr6	Gm6288	chr14	Gm8247
chr6	Gm7292	chr14	Gm8256
chr6	Hnrnpf	chr14	Gm8281
chr6	mmu-mir-7045	chr14	Gm9611
chr6	Pcbp1	chr14	Ints6
chr6	Tra2a	chr14	Micu2
chr6	Ube2h	chr14	Mir5131
chr6	Wbp11	chr14	Mphosph8
chr7	1700081H22Rik	chr14	Mtmr6
chr7	Aamdc	chr14	Nr1d2
chr7	Akt2	chr14	Ppp2r2a
chr7	Aspdh	chr14	Pxk
chr7	Atf5	chr14	Tmem254a
chr7	Atxn2l	chr14	Tmem254b
chr7	Bcam	chr14	Tmem254c
chr7	Catsperg1	chr14	Tsc22d1
chr7	Cdipt	chr14	Xkr6
chr7	Clpb	chr14	Zmym2
chr7	D430042O09Rik	chr15	1810049J17Rik
chr7	D830044I16Rik	chr15	2410089E03Rik
chr7	Dyrk1b	chr15	Azin1
chr7	E130304I02Rik	chr15	Ep300
chr7	Ercc1	chr15	Gm23880
chr7	Erf	chr15	Gm26884
chr7	Fus	chr15	Golph3
chr7	Galp	chr15	Gtpbp1
chr7	Gm5591	chr15	Lmbr1l
chr7	Gm6605	chr15	Muc19
chr7	Grik5	chr15	Nhp2l1
chr7	Gtf3c1	chr15	Nup50
chr7	Il4i1	chr15	Rad21
chr7	Josd2	chr15	Rgs22
chr7	Klc3	chr15	Ywhaz
chr7	Mapk1ip1	chr15	Zfr
chr7	Med25	chr16	Eaf2
chr7	mmu-mir-7052	chr16	Gm23935
chr7	Nup62	chr16	Golgb1
chr7	Pcf11	chr16	Golgb1
chr7	Pex11a	chr16	Lca5l

chr7	Pnmal2
chr7	Ppp1r37
chr7	Ppp2r2d
chr7	Rbbp6
chr7	Rsf1
chr7	Ube2s
chr7	Wdr93
chr7	Zc3h4
chr7	Zfp446
chr7	Zfp507
chr7	Zfp646
chr7	Zfp668
chr8	2610005L07Rik
chr8	4930467E23Rik
chr8	Acsl1
chr8	Agpat6
chr8	Amfr
chr8	Ap1g1
chr8	C330011M18Rik
chr8	Cdkn2aip
chr8	Cnep1r1
chr8	Csnk2a2
chr8	E030037K01Rik
chr8	Evi5l
chr8	Fam192a
chr8	Gm15319
chr8	Gm20946
chr8	Gm21092
chr8	Gm21119
chr8	Gm21769
chr8	Gm22291
chr8	Gm23284
chr8	Gm23647
chr8	Gm25212
chr8	Gm2716
chr8	Gm9725
chr8	Gtl3
chr8	n-R5s144
chr8	n-R5s146
chr8	n-R5s149
chr8	Rfx1
chr8	Rspry1
chr8	Smarca5
chr8	Tmem66
chr8	Usp38
chr8	Znrf1
chr9	4930535L15Rik
chr9	Arcn1
chr9	Dalrd3
chr9	Dennd4a

chr16	Mpv17l
chr16	Pdxdc1
chr16	Ppp1r2
chr16	Ptplb
chr16	Setd4
chr16	Ube2l3
chr16	Yeats2
chr17	Aars2
chr17	Agpat1
chr17	Atl2
chr17	AY036118
chr17	Btbd9
chr17	Dnah8
chr17	Dynlt1c
chr17	Fgfr1op
chr17	Flywch1
chr17	Gm16275
chr17	Gm17705
chr17	Gm20427
chr17	Gm26917
chr17	Gm26924
chr17	Hsp90ab1
chr17	mmu-mir-6968
chr17	Nfya
chr17	Oard1
chr17	Phf1
chr17	Phf10
chr17	Ppp1r2-ps1
chr17	Prrc2a
chr17	Rnf5
chr17	RP24-271E12.4
chr17	Rxrb
chr17	Slc39a7
chr17	Tagap1
chr17	Tbc1d22b
chr17	Tmem217
chr17	Trim39
chr17	Ube2i
chr17	Zfand3
chr18	Atp9b
chr18	Fam53c
chr18	Ndfip1
chr18	Pqlc1
chr18	Rnf138
chr18	Sil1
chr19	4930505N22Rik
chr19	9130011E15Rik
chr19	AI846148
chr19	Cfl1
chr19	Cnih2

chr9	Dnaja4
chr9	Elovl5
chr9	Fbxl12
chr9	Gm24083
chr9	Gm24270
chr9	Gtf2a2
chr9	Ift46
chr9	Ip6k1
chr9	Kif9
chr9	Klhl18
chr9	Map2k5
chr9	Map4
chr9	Mir425
chr9	mmu-mir-6236
chr9	Ndufaf3
chr9	Osbpl10
chr9	Pkm
chr9	Prdm10
chr9	Senp6
chr9	Sept7
chr9	Sltm
chr9	Ubl5
chr10	2510003E04Rik
chr10	4933403O03Rik
chr10	4933406P04Rik
chr10	4933408J17Rik
chr10	Ap3d1
chr10	Bclaf1
chr10	Btg1
chr10	Cirbp

chr19	Dpf2
chr19	Frat2
chr19	Gm15491
chr19	Hnrnpul2
chr19	Kdm2a
chr19	Lrrc10b
chr19	Mgea5
chr19	mmu-mir-8092
chr19	Naa40
chr19	Npm3
chr19	Pcgf6
chr19	Ppp1r2-ps3
chr19	Ppp6r3
chr19	Stip1
chr19	Suv420h1
chr19	Ttc9c
chr19	Zfp518a
chrX	Alg13
chrX	Asmt
chrX	Gm14819
chrX	Gm21887
chrX	Gm2825
chrX	Gm5073
chrX	Gm5123
chrX	Gm5755
chrX	Supt20-ps
chrY	Erdr1
chrY	Gm21572
chrY	Gm21599
chrY	Gm21780

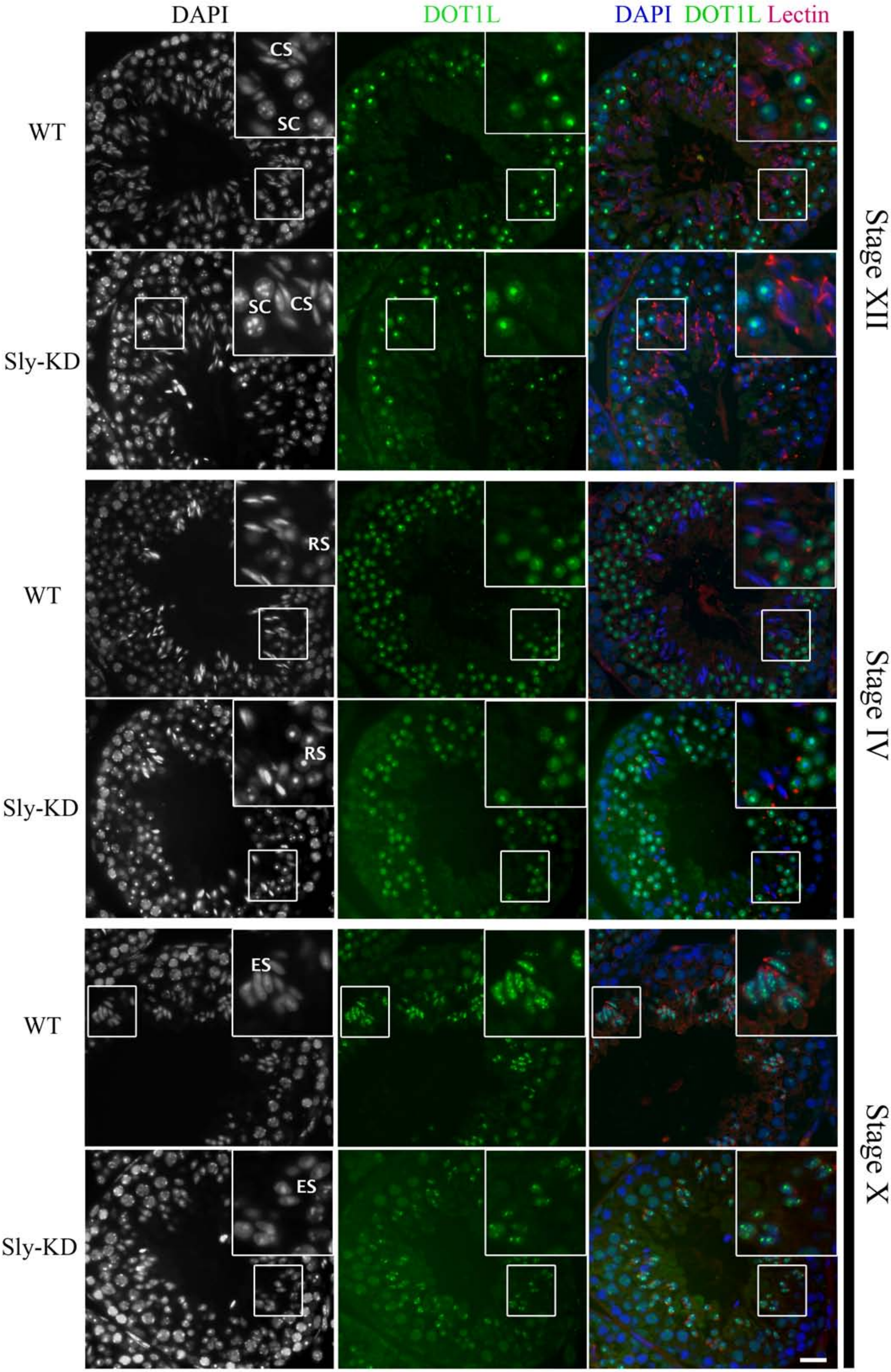
DAPI
DOT1L
DAPI DOT1L Lectin
WT
Sly-KD
WT
Sly-KD
WT
Sly-KD
CS
SC
SC
CS
RS
RS
ES
ES
Stage XII
Stage IV
Stage X

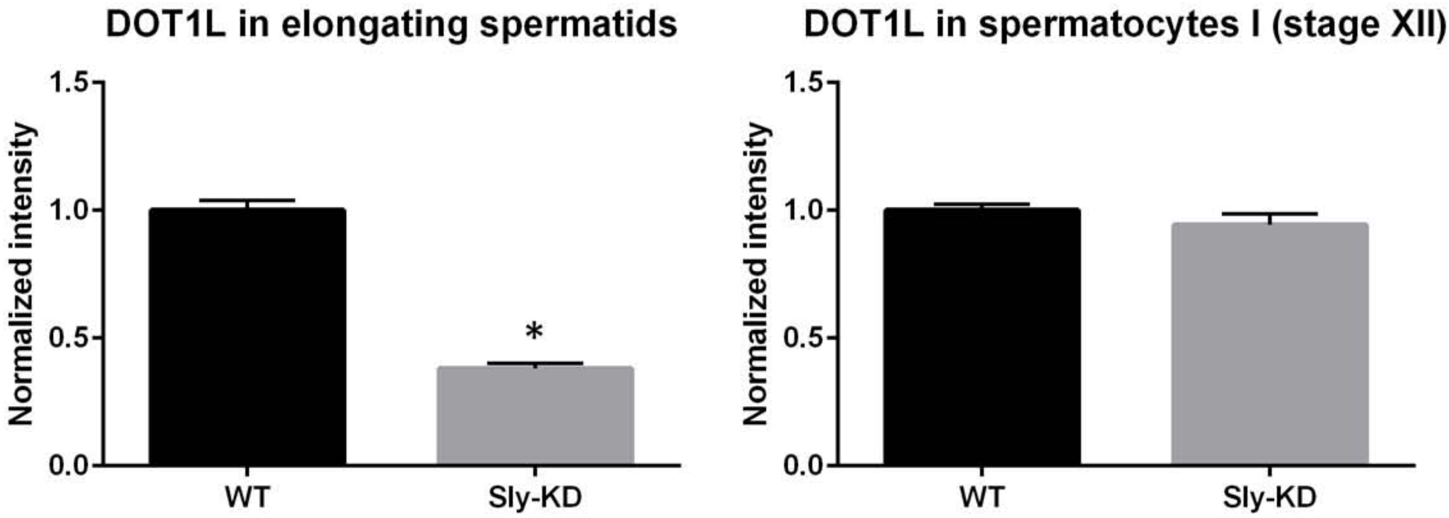
DOT1L in elongating spermatids
Normalized intensity
1.5
1.0
0.5
0.0
*
WT
Sly-KD
DOT1L in spermatocytes I (stage XII)
Normalized intensity
1.5
1.0
0.5
0.0
WT
Sly-KD

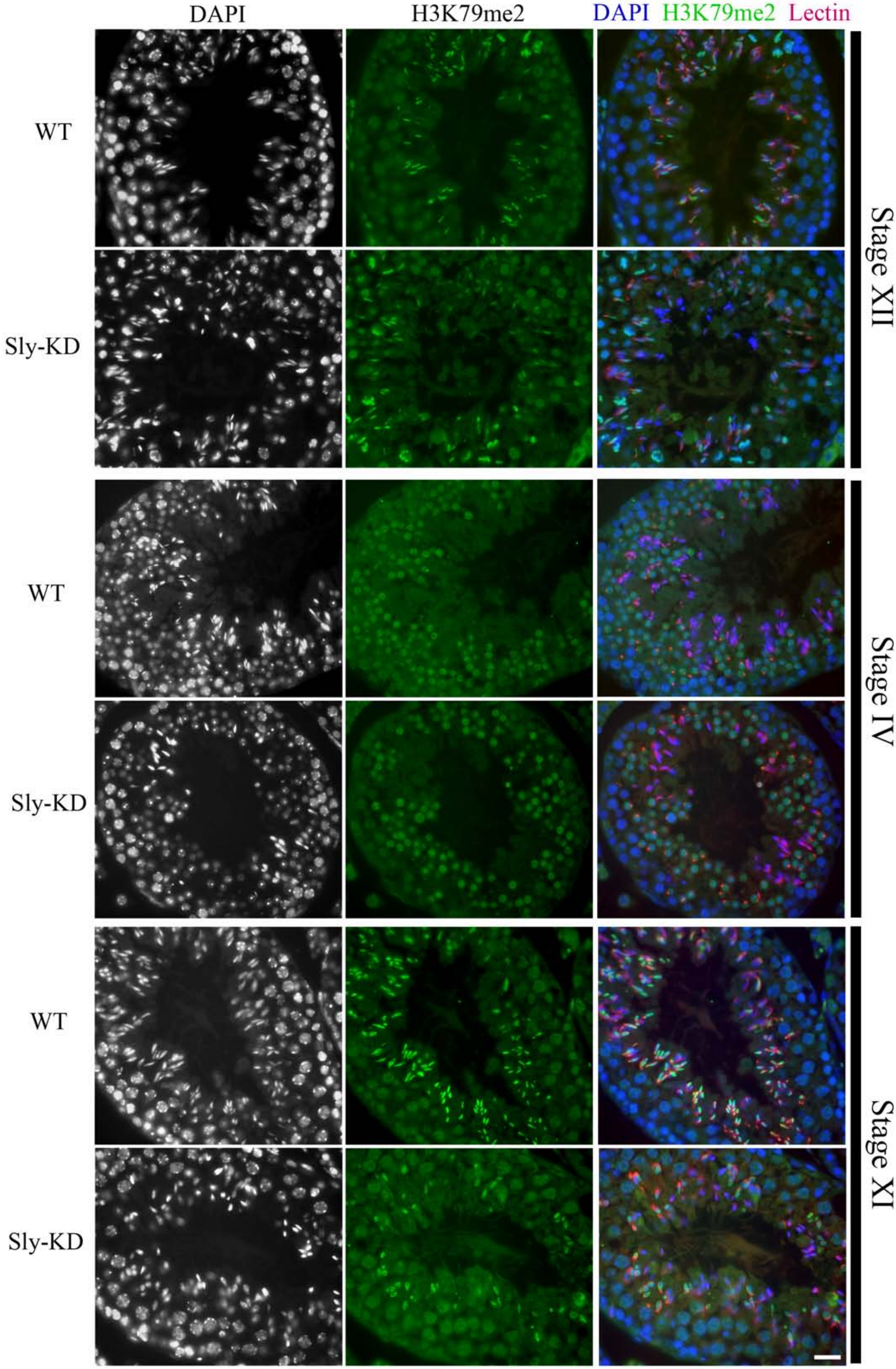
DAPI
H3K79me2
DAPI H3K79me2 Lectin
WT
Sly-KD
WT
Sly-KD
WT
Sly-KD
Stage XII
Stage IV
Stage XI

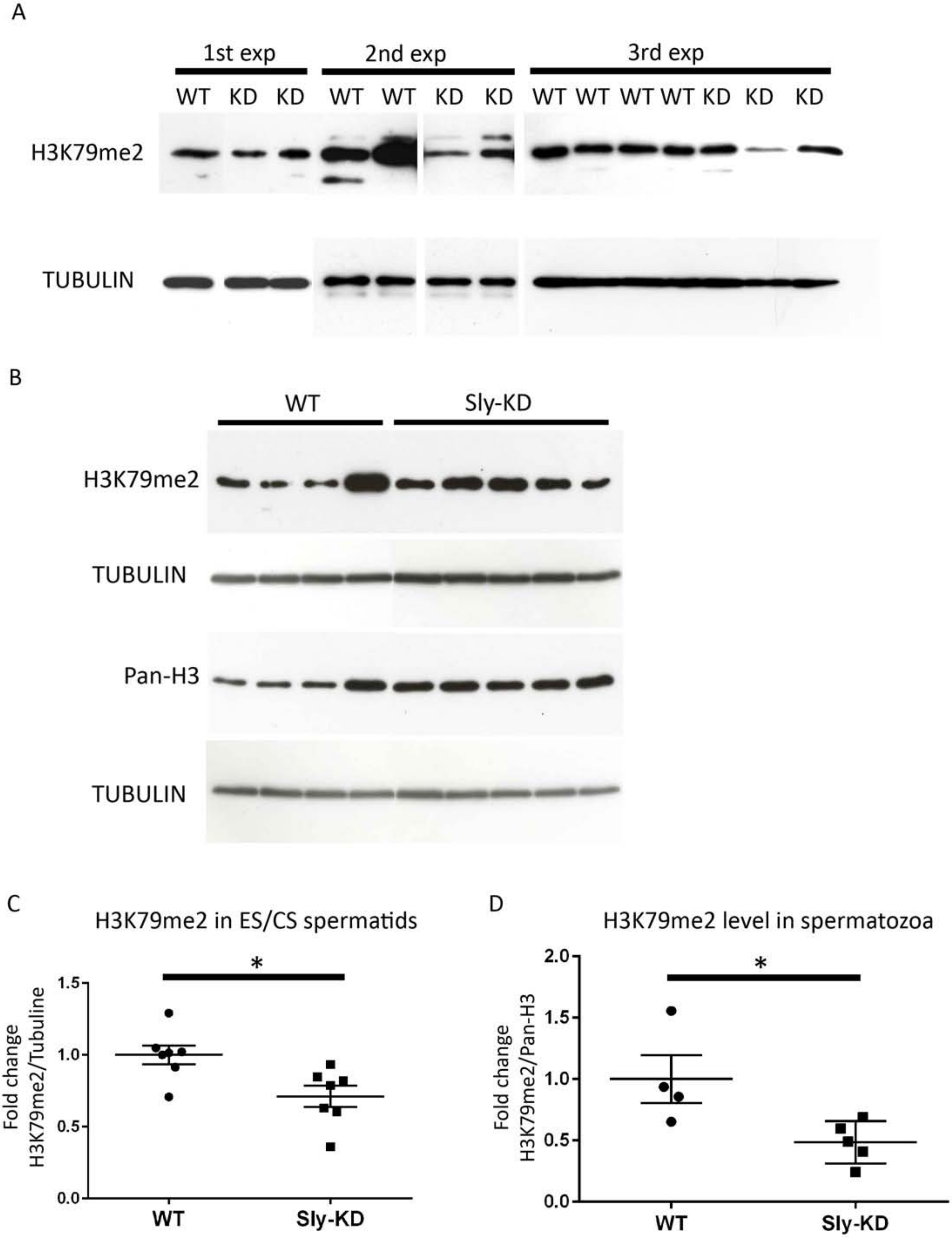
A
1st exp
2nd exp
3rd exp
WT KD KD WT WT KD KD WT WT WT WT KD KD KD
H3K79me2
TUBULIN
B
WT
Sly-KD
H3K79me2
TUBULIN
Pan-H3
TUBULIN
C
H3K79me2 in ES/CS spermatids
*
Fold change H3K79me2/Tubuline
1.5
1.0
0.5
0.0
WT
Sly-KD
D
H3K79me2 level in spermatozoa
*
Fold change H3K79me2/Pan-H3
2.0
1.5
1.0
0.5
0.0
WT
Sly-KD

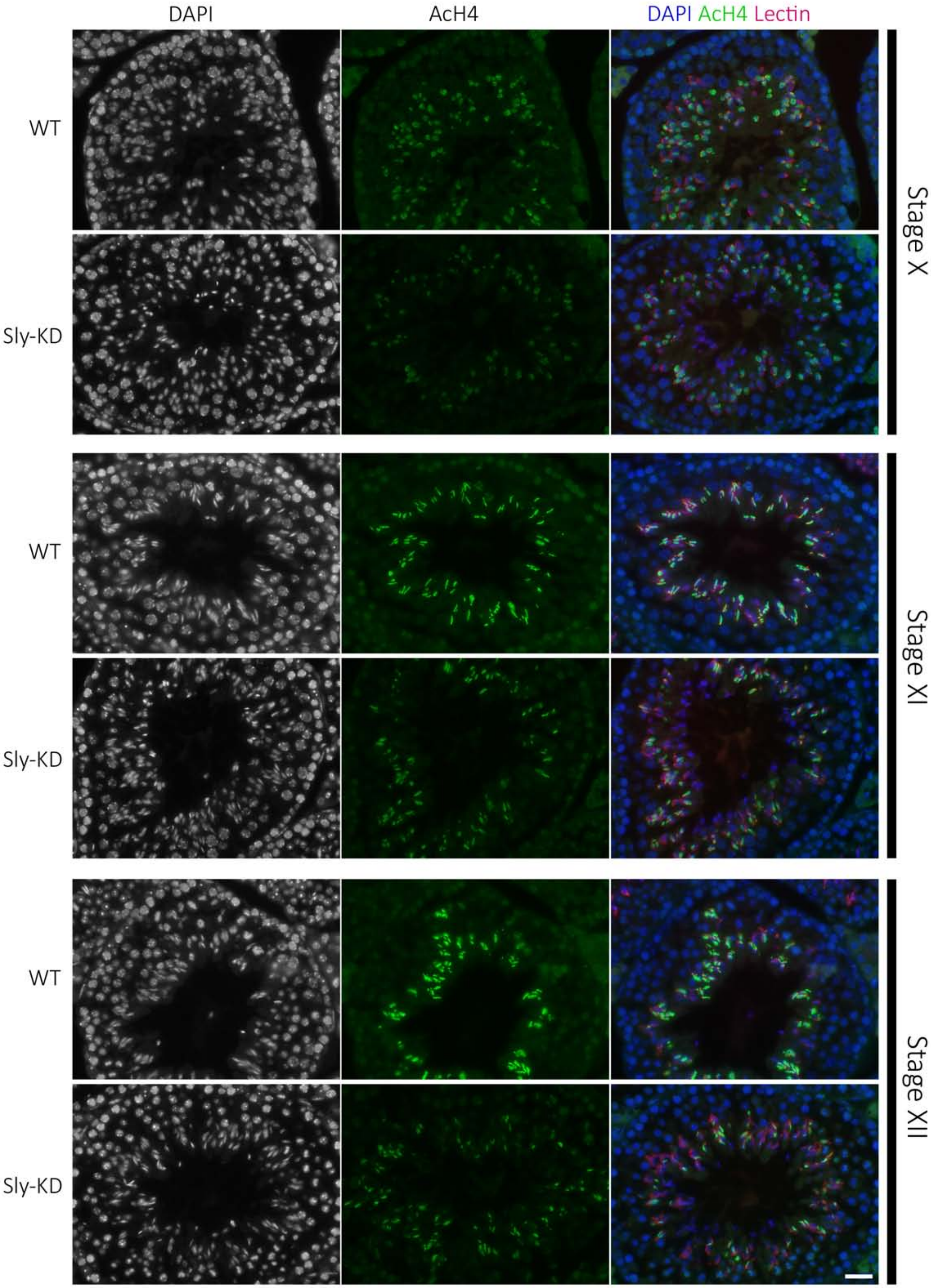
DAPI
AcH4
DAPI AcH4 Lectin
WT
Sly-KD
WT
Sly-KD
WT
Sly-KD
Stage X
Stage XI
Stage XII

Supplementary Figure 10 Moretti et al

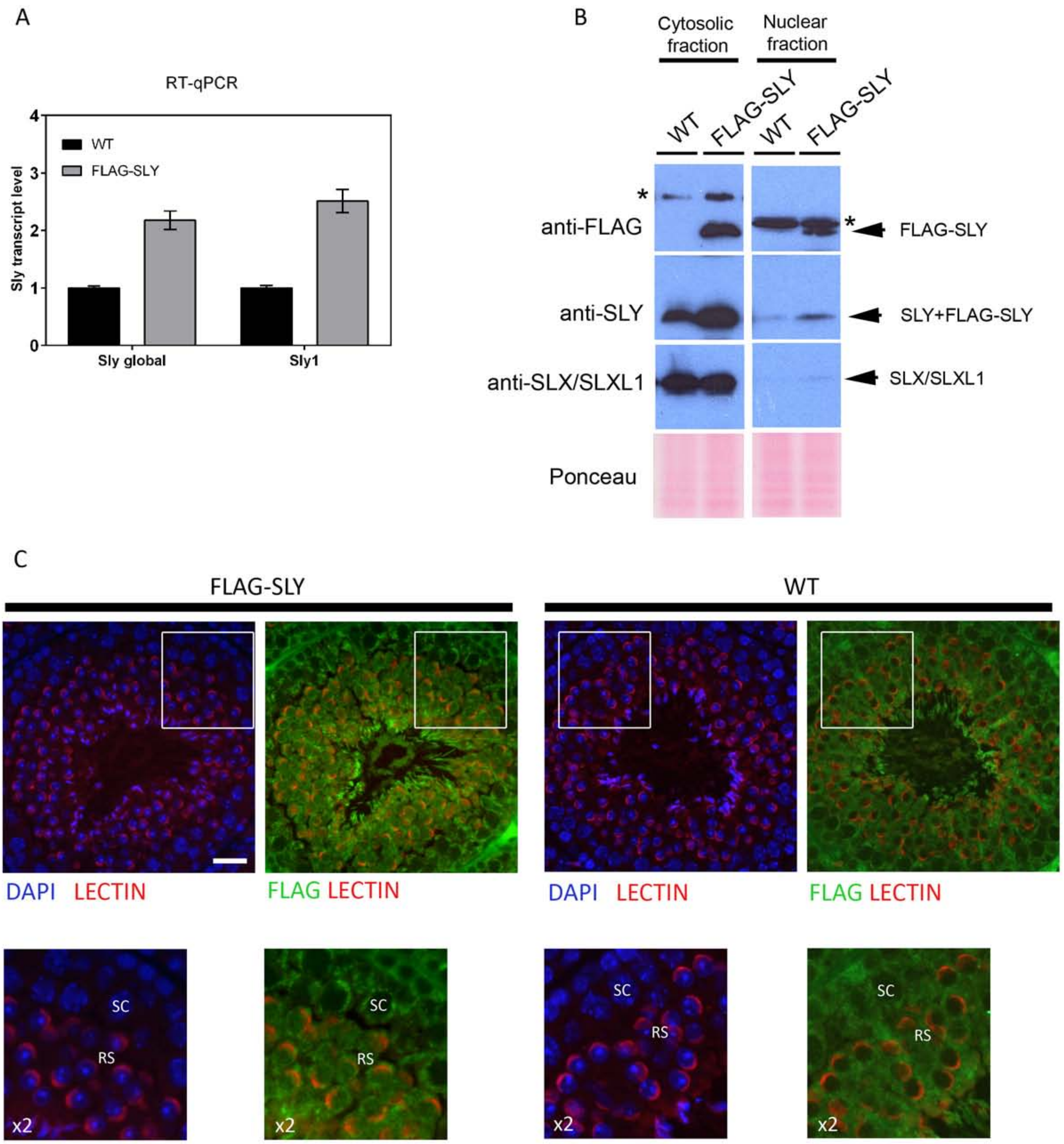

Supplementary Figure 11. List of primers designed for the study.

Primers used for RTqPCR

Gene	Primer sequence	Location	Annealing T°C
Gmcl1l	GCAGACTACAGCAATGCCTC ATCCCTGCAACTCAAGACCC	gene	60°C
Il2rg	GTTGGTTGGAACGAATGCCT CACTCCAGGCCGAAAAGTTC	gene	60°C
Dusp21	TGGTGCCCAGGAATCTAGTG TGGGTAGCTTGAGACGGAAA	gene	60°C
Spin2d	ACTATCTCTGGCAGCAGGAC GATCTGCTCCTCTGCCTCTT	gene	60°C
Rp2h	TGTGCCTAGCCTACCATCAG ATTATACCTGCCCTGCCAGC	gene	60°C
Ube2a	ACCGCGGACCCTGGTATATG CCAAAAATGACCGCATTCCA	gene	60°C
Ube2b	CGCCCCATCTGAAAACAACA TGGGACTCCATCGATTCTGC	gene	60°C
Kdm2a	CAGGTTGGATTCATGCTGTG GGATCGGTTGGTTATGCAGT	gene	60°C
Yeats2	TGTGGAAGTTAGAGAGCCCC TCAGGAACAACGCTCTGCTAC	gene	60°C
Ubb	ACTCTGCACTCTAGCCACTT GCTTACCATGCAACAAAACCT	gene	60°C
Mettl23	GCTGTAGTCCTGGCCCAATA GCAGCCAAAATCCCAGGAAG	gene	60°C
H2al3	AGCCAACATCAACAACCAGC GTCCAGGCATCTCGTCAAAC	gene	60°C

Primers used for ChIPqPCR

Name	Primer sequence	Location	Annealing T°C
SlxChIP	CATTCTTCCTACGCCACTCC CCTTAGGGTCCAACTTGTCG	TSS (420 bp downstream TSS)	55°C
RbmxChIP	ACAGGCCAAGGAAAGGAAAGT TCCTTTGTTCGCCCTCGTTG	TSS (42 bp downstream TSS)	55°C
Rhox11ChIP	GACCACTCTTGTGGTTTCCA AAGTTCTACCCCGTGTGTGC	TSS (flanking TSS)	55°C
Ctag2ChIP	CTTTCAAACAAAGGGCCCCA ATCTCCCCCTGTGTTGCTTTT	TSS (42 bp upstream TSS)	55°C
H2afb3ChIP	CAGAGTGCGATGTCACAGGA GTCCGGTACAAAGGGAGACA	TSS (8 bp upstream TSS)	55°C
Hist1h3aChIP	GAGGCTAAGGTAGTCTGCCG CTGGCCTACTCTCCTTCAATGT	TSS (118bp upstream TSS)	55°C
Jmjd1cChIP	ATCCCTGGAAAACGGCAGAT ACTTCCCGTCCAATCACAACA	TSS (850bp upstream TSS)	55°C
Dot1lChIP	GGGATTCCTTGCCTTTCGTG CCCCTGACTTCCTAGGGTTCT	TSS (541 bp downstream TSS)	55°C
NC	TGGCATTGTGGGCTAGATTT TGGAGATAAGATATGCGTCAAG	intragenic (170kb downstream TSS)	55°C
Ep300ChIP	AAACTCTCATCTCCGGCCCT AGCACCCTGGAATGAAGGTG	TSS (463 bp downstream TSS)	55°C
Rdm1ChIP	CAACCAAAACTTCTCGGCCTC CCCCATACACTCAACACCGA	TSS (flanking TSS)	55°C
Prr13ChIP	GCAACGGTTTCCTCCTTGTT TCAGTCTGGGTTCGCACTTC	TSS (35 bp downstream TSS)	55°C